Metal-Substituted Bacteriochlorophylls. 1. Preparation and Influence of Metal and Coordination on Spectra

ARTICLE *in* JOURNAL OF THE AMERICAN CHEMICAL SOCIETY · APRIL 1998

Impact Factor: 12.11 · DOI: 10.1021/ja970874u

Metal-Substituted Bacteriochlorophylls. 1. Preparation and Influence of Metal and Coordination on Spectra

Gerhard Hartwich,[†,‡] Leszek Fiedor,[§,⊥,∥] Ingrid Simonin,[‡] Edmund Cmiel,[†] Wolfgang Schäfer,[⊗] Dror Noy,[§,#,∥] Avigdor Scherz,[§] and Hugo Scheer*[,‡]

Contribution from the Institut für Physikalische und Theoretische Chemie, Technische Universität München, D-85748 Garching, Germany, Botanisches Institut der Universität, D-80638 München, Germany, Department of Plant Sciences, Weizmann Institute of Science, 76100 Rehovot, Israel, and Max-Planck-Institut für Biochemie, D-82152 Martinsried, Germany

Received March 19, 1997. Revised Manuscript Received October 29, 1997

Abstract: In contrast to porphyrins and chlorins, the direct metalation of bacteriochlorins is difficult. Nevertheless, Cu^{2+} and Zn^{2+} can be introduced into bacteriopheophytin in acetic acid, whereas Cd^{2+} can be inserted in dimethylformamide. The former reactions depend on the substituents of the isocyclic ring: they are facilitated if enolization of the β-ketoester system is inhibited. Starting with [Cd]-bacteriochlorophyll-a or its 13^2-hydroxy derivative, a series of metallo-bacteriochlorins with central divalent ions Pd^{2+}, Co^{2+}, Ni^{2+}, Cu^{2+}, Zn^{2+}, and Mn^{2+} have been obtained by transmetalation. Like in the parent Mg complex, the four principal optical transitions are well-separated in these complexes, and their responses to changes in the central metal and its coordination state can be followed in detail. The energies of the Q_y and B_x transitions are almost independent of the central metal, whereas the Q_x and B_y transition energies change significantly, depending on the central metal as well as the presence of additional axial ligands. If the complexes are grouped by their coordination number, empirical linear correlations exist between these shifts and the ratio χ_M^P/r_M^i, where χ_M^P is Pauling's electronegativity value and r_M^i is the ionic radius of the metal. A similar correlation was found for those ^{1}H NMR signals influenced mainly by the ring current and for the redox potentials. This observation was in contrast with the linear relationships with χ_M^P alone, found for metal-substituted porphyrins. The spectral variations influenced by the central metal and its state of ligation are attributed, within the framework of the four-orbital model, to the electrostatic interaction of the electron densities in the four orbitals with the effective charge of the central metal ions, which is most pronounced for the a_{2u} orbital (HOMO-1). Ligation studies have revealed that addition of the first axial ligand decreases the effective charge of the central metal by approximately 50% and addition of the second axial ligand by another 20% with respect to the absence of axial ligands. The singlet−triplet splitting deduced from fluorescence and phosphorescence measurements is similar for [Pd]-, [Cu]-, [Zn]-, and [Mg]-BChl (4550 ± 100 cm^{-1}).

Introduction

The Mg-containing (bacterio)chlorophylls ((B)Chl) and their free bases, the (bacterio)pheophytins ((B)Phe), are essential to photosynthesis. They act as light-harvesting or as redox pigments enabling light-induced charge separation within the reaction center.[1] The pigments are also potentially useful photosensitizers, e.g., in photodynamic tumor therapy.[2−7] Complexes of cyclic tetrapyrroles with metals other than Mg were studied in the chlorin[8,9] (17,18-dihydroporphyrin) and especially in the porphyrin[10−13] series to better understand their spectroscopic and redox properties. These complexes show a linear relationship between the electronegativity (χ_M^P; Pauling values) of the central metal and the redox potential.[9] Interpretation of the optical spectra has been less straightforward,[10−12] mostly because of insufficient experimental information. The electronic

* Author to whom correspondence should be addressed.
† Technische Universität München.
‡ Botanisches Institut der Universität.
§ Weizmann Institute of Science.-
⊥ Current address: Institute of Molecular Biology, Jagiellonian University, PL-31-120 Cracow, Poland.
In partial fulfillment of M.Sc. Thesis.
∥ In partial fulfillment of Ph.D. Thesis.
⊗ Max-Planck-Institut für Biochemie.

(1) For leading references, see: *Chlorophylls*; Scheer, H., Ed.; CRC Press: Boca Raton, FL, 1991.
(2) Spikes, J. D.; Bommer, J. C. In *Chlorophylls*; Scheer, H., Ed.; CRC Press: Boca Raton, FL, 1991; pp 1181−1204.
(3) Pandey, R. K.; Bellnier, D. A.; Smith, K. M.; Dougherty, T. J. *Photochem. Photobiol.* **1990**, *53*, 65−72.
(4) Pandey, R. K.; Shiau, F. Y.; Sumlin, A. B.; Dougherty, T. J.; Smith, K. M. *Bioorg. Med. Chem. Lett.* **1994**, *4*, 1263−1267.
(5) Moser, J. G.; Suchomski, R.; Danielowski, T.; Wagner, B.; Scheer, H.; Hartwich, G. *SPIE Proceedings of the 5th Biennal Meeting IPA, Amelia Island FA* **1995**, *2371*, 178−186.
(6) Rosenbach-Belkin, V.; Chen, L.; Fiedor, L.; Tregub, I.; Pavlotsky, F.; Brumfeld, V.; Salomon, Y.; Scherz, A. *Photochem. Photobiol.* **1996**, *64*, 174−181.
(7) Boyle, R. W.; Dolphin, D. *Photochem. Photobiol.* **1996**, *64*, 469−485.
(8) Hyninnen, P. H. In *Chlorophylls*; Scheer, H., Ed.; CRC Press: Boca Raton, FL, 1991; pp 145−209.
(9) Watanabe, T.; Kobayashi, M. In *Chlorophylls*; Scheer, H., Ed.; CRC Press: Boca Raton, FL, 1991; pp 282−316.
(10) Fajer, J.; Barkiga, K. M.; Smith, K. M.; Zhong, E.; Gudowska-Nowak, E.; Newton, N. D. In *Reaction Centers of Photosynthetic Bacteria*; Michel-Beyerle, M. E., Ed.; Springer-Verlag: Berlin, 1990; pp 367−376.
(11) Barkiga, K. M.; Chantranupong, L.; Smith, K. M.; Fajer, J. *J. Am. Chem. Soc.* **1988**, *110*, 7566−7567.
(12) Renner, M. W.; Zhang, Y.; Noy, D.; Scherz, A.; Smith, K. M.; Fajer, J. In *Reaction Centers of Photosynthetic Bacteria*; Michel-Beyerle, M. E., Ed.; Springer-Verlag: Berlin, 1996; pp 367−376.
(13) Buchler, J. W. In *Porphyrins and Metalloporphyrins*; Smith, K. M., Ed.; Elsevier: New York, 1975; pp 157−232.

S0002-7863(97)00874-3 CCC: $15.00
Published on Web 04/02/1998

transitions are pairwise degenerate in metallo-porphyrins ($E_{Q_x} \approx E_{Q_y}$, $E_{B_x} \approx E_{B_y}$). In metallochlorins, the visible bands (Q_x and Q_y) are well-separated, but Q_x is often hardly discernible, and the B bands are again (nearly) degenerate.

Compared to the chlorins (chlorophylls), bacteriochlorins (7,8,17,18-tetrahydroporphyrins) and, in particular, bacteriochlorophylls are of potential advantage because all of their four $\pi-\pi^*$ transitions predicted by the four-orbital model are well separated.[14,15] However, limited information has been available about bacteriochlorins with central metals other than Mg.[4,16,25]

We have found that direct metalation methods for chlorins[8,26] were successful with only a few metals when applied to the free base analogues of bacteriochlorins, the bacteriopheophytins.[16a,17,25] However, Strell and Urumov's principle of transmetalation[27] to indirectly prepare different metal-substituted chlorins could be adapted for preparing additional metal-substituted bacteriochlorophylls ([M]-BChl). Starting from [Cd]-BChl (**8a**, or its 13^2-OH derivative, **8b**), Pd^{2+}, Co^{2+}, Ni^{2+}, Cu^{2+}, Zn^{2+}, and Mn^{2+} were incorporated into BPhe (**1a**,**b**), to yield the pigments **2a**,**b** to **6a**,**b** and **9a**,**b** (Figure 1).

The redox chemistry,[19,22,28] EXAFS spectra,[23] and incorporation of some of these complexes into bacterial reaction centers has been independently reported.[17,18,20,21,24] Here we describe their preparation and spectral characterization, and we present a correlation between their physical properties and the characteristic parameters of the central metal. A quantitative analysis of the data based on electrostatic interactions between the metal and all the negative and positive (partial) charges on the macrocycle in the frontier orbitals is the subject of the following paper.[28]

Results and Discussion

Preparation. Besides the Cd necessary to form the precursor complex for the transmetalation, only Cu and Zn could be introduced into BPhe or BChl in reasonable yields by direct methods.[17,25] Although the metalation of BPhe with Zn^{2+} or Cd^{2+} by the acetate/dimethylformamide (DMF) method (Experimental Section) is almost independent of modifications at the macrocycle, the conditions for the acetic acid method (Experimental Section) used to achieve metalation with Cu (or Zn) strongly depend on the substituents at position C-13^2.

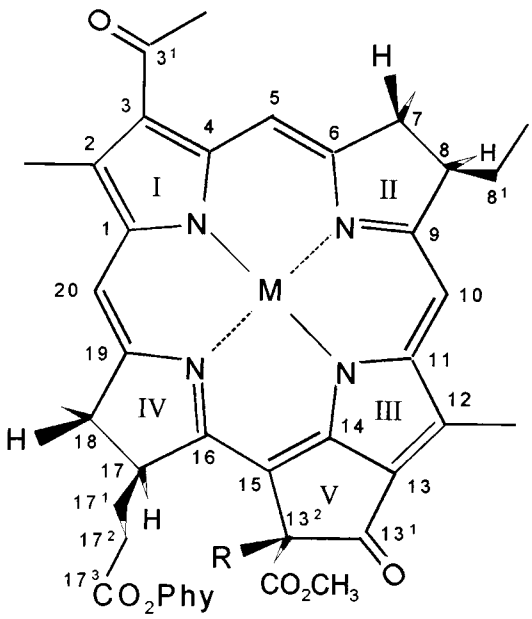

Compound	1	2	3	4	5	6	7	8	9
M	2H	Pd	Co	Ni	Cu	Zn	Mg	Cd	Mn

Figure 1. Structure formulas. a and b after the numbers indicate R = H and R = OH, respectively. Phy = phytyl ($C_{20}H_{39}$).

Low yields were observed for the metalation of BPhe (BChl) with Cu^{2+} in acetic acid when the reaction mixture was stirred for several hours at 20 °C; at 100 °C the reaction was completed within 15 min with a 90% yield. In contrast, incorporation of Cu^{2+} into 13^2-hydroxy-BPhe to yield **5b** was already completed in 10 min at ambient temperature. Since 13^2-hydroxylation inhibits enolization of the BPhe β-ketoester system of ring V, the reaction was also tested with 13^2-decarbomethoxy-BPhe, which lacks these chelating substituents. Again, metalation was as fast as for 13^2-hydroxy-BPhe. Incorporation of Zn^{2+} into the different BPhe derivatives by the acetic acid method resulted in a similar although less pronounced kinetic difference. Metalation of BPhe (or BChl) by Zn^{2+} was completed after 120 min of reflux at 100 °C, and that of the 13^2-derivatives after 30 min.

We propose that the kinetic differences observed in applying the acetic acid method reflect the release rate of the central protons of BPhe prior to or simultaneous to metal incorporation (the rate-determining step).[29] However, the functioning of metalation in acetic acid is surprising but may be explained by a catalytic effect: acetic acid protonates the conjugated keto

(14) Gouterman, M.; Wagnière, G. H.; Snyder, L. C. *J. Mol. Spectrosc.* **1963**, *11*, 108−127.
(15) Hanson, L. K. In *Chlorophylls*; Scheer, H., Ed.; CRC Press: Boca Raton, FL, 1991; pp 993−1041.
(16) (a) Losev, A. P.; Knyukshto, V. N.; Kochubeeva, N. D.; Solovev, K. N. *Opt. Spectrosc.* **1991**, *97*, 97−101. This method did not work for us. (b) Donohoe, R. J.; Frank, H. A.; Bocian, D. F. *Photochem. Photobiol.* **1988**, *48*, 531−537.
(17) Hartwich, G. Dissertation Thesis, Technical University of München, 1994.
(18) Hartwich, G.; Friese, M.; Ogrodnik, A.; Scheer, H.; Michel-Beyerle, M. E. *Chem. Phys.* **1995**, *197*, 423−434.
(19) Hartwich, G.; Geskes, C.; Scheer, H.; Heintze, J.; Mäntele, W. *J. Am. Chem. Soc.* **1995**, *117*, 7784−7790.
(20) Hartwich, G.; Scheer, H.; Aust, V.; Angerhofer, A. *Biochim. Biophys. Acta* **1995**, *1230*, 97−113.
(21) Scheer, H.; Hartwich G. In *Anoxygenic Photosynthetic Bacteria*; Blankenship, R. E., Madigan, M. T., Bauer, C. E., Eds.; Kluwer: Dordrecht, 1995; pp 649−664.
(22) Geskes, C.; Hartwich, G.; Scheer, H.; Mäntele, W.; Heintze, J. *J. Am. Chem. Soc.* **1995**, *117*, 7776−7783.
(23) Chen, L.; Wang, Z.; Hartwich, G.; Katheder, I.; Scheer, H.; Tiede, D. M.; Scherz, A.; Montano, P. A.; Norris, J. R. *Chem. Phys. Lett.* **1995**, *234*, 437−444.
(24) Frank, H.; Chynwat, V.; Hartwich, G.; Meyer, M.; Katheder, I.; Scheer, H. *Photosyn. Res.* **1993**, *37*, 193−203.
(25) Fiedor, L. Ph.D. Thesis, The Weizmann Institute of Science, Rehovot, Israel, 1994.
(26) For leading references, see: Dolphin, D., Ed. *The Porphyrins*; Academic: New York, 1979; Vol. III, IV.
(27) Strell, M.; Urumov, T. *Liebigs Ann. Chem.* **1977**, 970−974.
(28) Noy, D.; Fiedor, L.; Hartwich, G.; Scheer, H.; Scherz, A. *J. Am. Chem. Soc.* **1998**, *120*, 3684−3693.

(29) Besides this intuitive mechanism, also other, more complex mechanisms may account for the observed differences in the rate of metalation by the acetic acid method, but some of them can be ruled out. For instance, complexation of the metal ions to the isocyclic carbonyls that may act as a bidentate ligand can explain the low reactivity of BPhe. However, significant variations in the Q_y transition should accompany such complexation (ref 56). Since no such spectral changes were observed during the insertion of Cu^{2+} and Zn^{2+}, this mechanism can be ruled out. Another explanation could be that the BPhes modified at C-13^2 are more amenable to the steric distortions required for the formation of an intermediate sitting atop (SAT) the complex (ref 30). However, the steric effects around the C-13^2 do not seem to play an important role, since 13^2-decarbomethoxy and 13^2-hydroxy derivates exhibit similar reactivities in the metalation reaction. Furthermore, such distortions are also expected to affect the BPhe optical absorption (ref 10), in contrast to what has been observed in our experiments.

Table 1. Spectral Properties of Natural and Transmetalated Pigments **1a**,**b**−**9a**,**b**[a]

compd (^{1}H NMR)[e]	absorption[b] λ_{max} [nm] (ϵ [10^3 M^{-1} cm^{-1}])				emission[c] λ_{max} [nm]	χ_M/r^i_M [d]	FAB-MS mol ion
	B_y	B_x	Q_x	Q_y			
1a (+)[e]	356 (113)	383 (62.7)	525 (28.3)	750 (67.5)	759		
	362 (92.3)	*389 (49.3)*	*532 (26.2)*	*754 (56.4)*			
2a (+)[h]	331 (43.6)	383 (37.2)	529 (14.5)	753 (92.0)	764 (755)	[3.44]	992 (^{106}Pd)
	334 (33.7)	*388 (27.8)*	*535 (13.5)*	*763 (61.5)*			
3a (−)	336 (34.8)	388 (27.1)	531 (8.9)	766 (63.7)	*f*	[3.21][g]	945 (^{59}Co)
	355 (40.6)	*386 (27.5)*	*562 (10.2)*	*767 (56.3)*			
4a (−)[g]	335 (45.7)	390 (30.4)	531 (11.4)	779 (63.0)	*f*	[3.18], 2.86	944 (^{58}Ni)
	366 (49.2)	*391 (30.3)*	*598 (16.1)*	*771 (71.8)*			
5a (−)	342 (53.3)	390 (42.9)	538 (14.5)	771 (64.1)	*f*	[3.06]	949 (^{63}Cu)
	358 (44.7)	*395 (31.9)*	*573 (12.2)*	*780 (56.1)*			
6a (+)	353 (58.9)	389 (39.7)	558 (18.0)	762 (67.7)	782 (772)	[2.48]	950 (^{64}Zn)
	364 (52.4)	*390 (31.7)*	*579 (16.5)*	*773 (57.1)*			
7a (+)	357 (73.3)	390 (48.0)	573 (20.8)	771 (91.0)	788 (778)	1.82	910 (^{24}Mg)
	374 (57.7)	*not resolved*	*612 (16.9)*	*781 (76.0)*			
8a (+)	359 (80.3)	389 (53.5)	575 (22.3)	761 (88.3)	778 (774)	1.78	1000 (^{114}Cd)
	368 (65.6)	*391 (44.1)*	*593 (19.4)*	*773 (69.6)*			
9a (−)	362 (71.8)	392 (43.0)	587 (18.0)	770 (76.7)	*f*	1.89	941 (^{55}Mn)
	373 (64.4)	*not resolved*	*601 (16.4)*	*780 (66.0)*			

[a] The absorption and fluorescence spectra of the 13^2-OH pigments (**1b**−**9b**) matched those of the respective 13^2-H parent compounds, except for a systematic blue shift of the Q_x absorption by ∼5 nm. The mass spectra were always shifted by 16 mass units to higher values. All wavelengths are in [nm]. [b] Absorption and extinction coefficients (by AAS) at 298 K in DE (upper line) and pyridine (lower line, *italics*). [c] Fluorescence in DE/petroleum ether/2-propanol (5:5:2; v/v/v) at 298 K (77 K). [d] Electronegativity (χ_M) and effective ionic radii (r^i_M in 10^{-14} m) for 6-fold coordination (data in brackets use radii for 4-fold coordination) from ref 13. If data used in Figure 3 are attributed to different coordination numbers, the radii were estimated using a 5% increased r^i_M per additional ligand.[43,49] [e] ^{1}H NMR in pyridine-d_5: (+) = sharp signals, (−) = extensive line broadening because of paramagnetic central metal. [f] Not fluorescent (Spex fluorolog 221). [g] Sharp ^{1}H NMR signals in C^2H_3CN. [h] Pd analysis is error prone. It can be both be grossly underestimated, and ϵ accordingly overestimated, by incomplete removal of Pd from the macrocycle, or overestimated (= ϵ underestimated) by band overlap (Kälin, Scheer, and Schraml, unpublished results).

groups at position C-13^1 and/or C-3^1, thereby increasing the s-character and acidity of the N-atoms of ring I or III or both. Reducing the acidity of the amino nitrogens is expected to lower the rate and yield of metal insertion. Such a reduction is possible when the catalytic effect of protonation at C-13^1 is suppressed by acid-induced 13^1-13^2-enol formation, which is only possible when an enolizable proton at C-13^2 is present. Thus demethoxycarbonylation (pyrolysis) as well as hydroxylation of BPhe increases the acidity of the amino nitrogens which should result in an observed acceleration of the metalation process. The idea of amino-deprotonation as a rate-determining step for direct metalation by the acetic acid method is confirmed by the observation that reaction kinetics become almost independent of the substitution at C-13^2 when DMF is used as a solvent and by its ease of transmetalation. For metalation in DMF, the catalytic effect of protonation is switched off, and for transmetalation, no protonation is necessary.

The [Cd] complexes are readily accessible by the acetate/DMF method and can be transmetalated with excellent yield to the other metal complexes under mild conditions (Experimental Section). The easy transmetalation using [Cd]-BChl as a precursor is unexpected and is probably due in part to the large ionic radius (r^i_M) of Cd^{2+} (95 pm) compared to Mg^{2+} (r^i_M = 72 pm). It is assumed that Cd does not fit into the "inner hole" spanned by the four nitrogens of the macrocycle and that it forms a sitting-atop complex.[30] This is supported by the low stability of the Cd complex, which already demetalates at pH 6−7. Another factor is the solvent (acetone) in combination with the counterion (chloride) of the metal used for the reaction. During transmetalation, $CdCl_2$ and [M]-BChl are formed in equilibrium with the reactands, and the very low solubility of $CdCl_2$ in acetone causes its removal and shifts the equilibrium to the side of the end products.

All end products were characterized by absorption, fluorescence, ^{1}H NMR, and FAB-mass spectroscopy (FAB-MS) (Tables 1 and 2). The Mn^{2+} and Co^{2+} oxidation states, under the experimental conditions, were confirmed by spectroelectrochemical measurements: Mn^{2+}/Mn^{3+} oxidation occurs in **9a**,**b** at −0.07 V vs Ag/AgCl and Co^{2+}/Co^{1+} reduction in **3a**,**b** at −1.04 V.[19,22] These values were similar to data obtained for other metallo-porphyrins.[31] The spectral changes were as expected for metal-centered redox reactions and provided no indication of π-cation (Mn) or π-anion (Co) radical formation.

Table 2. ^{1}H NMR Data for Diamagnetic Metal-Substituted Bacteriochlorophylls in Pyridine-d_5. Chemical Shifts in ppm against Tetramethylsilan for Some Selected Protons

proton	[Ni]-BChl[a]	[Pd]-BChl	[Zn]-BChl	BChl	[Cd]-BChl
5-H	8.64	9.59	9.45	9.52	9.33
10-H	8.21	8.74	8.67	8.64	8.60
20-H	8.08	8.62	8.55	8.50	8.45
17-H		4.25	4.20	4.21	4.20
18-H		4.37	4.35	4.33	3.42
2-CH_3	3.09	3.38	3.47	3.45	3.42
13^2-CO_2CH_3	3.64	3.89	3.81	3.78	3.78
13^2-H	5.60	6.49	6.52	6.56	6.59
12-CH_3	3.23	3.43	3.52	3.56	3.56
3-$COCH_3$	2.92	3.07	3.11	3.12	3.10

[a] Solvent C^2H_3CN (extensive line broadening in pyridine-d_5 because of paramagnetic high-spin Ni^{II}).

The FAB-MS spectra exhibited the expected molecular ions and isotopic distributions. The fragmentation was similar for all [M]-BChls investigated. Fragments with highest atomic mass unit (amu) arose from the loss of the phytyl residue (−280 amu), followed by a fragment, which in addition, was decarbomethoxylated at position C-13^2 (−338 amu). The 13^2-hydroxylated complexes (**1b**−**9b**) showed all major peaks shifted by +16 amu.

Emission Spectra. The fluorescence emissions in a mixture of diethyl ether (DE)/petroleum ether/2-propanol (5/5/2, v/v/v)

(30) Hambright, P. In *Porphyrins and Metalloporphyrins*; Smith, K. M., Ed.; Elsevier: New York, 1975; pp 233−278.
(31) Davis, D. G. In *The Porphyrins*; Dolphin, D., Ed.; Academic: New York, 1979; Vol. IV, pp 127−152.

at 77 and 298 K (Table 1) that can be detected ($\Phi_F > 10^{-3}$) can be attributed to the respective complexes by their fluorescence excitation spectra. The Stokes shifts of all fluorescent complexes were similar (260 ± 70 cm^{-1}) and almost metal- and temperature-independent.

At 298 K, phosphorescence was detectable for [Cu]-BChl at ~1230 nm and for [Pd]-BChl at 1170 nm.[32] The difference between the fluorescence and phosphorescence energies of [Pd]-BChl corresponds to a singlet−triplet energy splitting of ΔE_{ST} = (4530 ± 70) cm^{-1}. [Cu]-BChl did not show any detectable fluorescence. Assuming a Stokes shift similar to that of the other complexes, the hypothetical fluorescence was estimated at 787 nm, which gives ΔE_{ST} = (4580 ± 70) cm^{-1}. Phosphorescence for both complexes was recorded in toluene, in which the complexes showed absorption maxima that are almost identical to those in DE or DE/petroleum ether/2-propanol. Both complexes should be four-coordinated in these solvents with no additional axial ligand as indicated by the correlation between absorption spectra and coordination discussed below.

The singlet−triplet splitting energies for four-coordinated [M]-BChl are of a size similar to those of natural BChl in its 5-fold (ΔE_{ST} = 4610 cm^{-1}) or 6-fold coordination state (ΔE_{ST} = 4550 cm^{-1}), as well as that of [Zn]-BChl in different solvents (ΔE_{ST} = 4550−4600 cm^{-1}).[33] In this series of metal-substituted BChls, the singlet−triplet splitting energies are then almost independent (ΔE_{ST} = 4500−4600 cm^{-1}) of the central metal and of its state of ligation.

UV/Vis Absorption. The UV/vis absorption spectra of all complexes show four distinct bands labeled B_y, B_x, Q_x, and Q_y in order of decreasing transition energy, and they resemble those of BChl and BPhe. These bands show a characteristic pairwise dependence when the central metal is changed: the B_x and Q_y transition energies are only slightly affected by changing the central metal or its coordination. In contrast, strong and distinct shifts are seen for the B_y and Q_x bands. Replacing Mg by Ni, for example, results in blue shifts of 1750 and 1400 cm^{-1} in the B_y and Q_x bands, respectively, whereas the B_x and Q_y bands are shifted by less than 150 cm^{-1}. Large shifts for Q_x and B_y and minor shifts for B_x and Q_y are also seen for the other metals (Table 1).

The large shifts of Q_x and B_y can be rationalized qualitatively by the four-orbital model.[14,15,34,35] According to this model the UV/vis spectra result from transitions among the four orbitals: a_{2u} (HOMO-1), a_{1u} (HOMO), e_{gx} (LUMO), and e_{gy} (LUMO+1).[36] In a zero-order approximation neglecting configuration interaction, B_y is a transition from a_{2u} to e_{gy}, B_x from a_{1u} to e_{gy}, Q_x from a_{2u} to e_{gx}, and Q_y from a_{2u} to a_{1u}.[15] The a_{2u} orbital has high electron densities at the four nitrogens nearest to the metal in the "inner hole" of the porphyrin system, whereas the e_{gx} and e_{gy} orbitals have substantial electron densities on only two nitrogens and the a_{1u} orbital has almost no electron density at the nitrogens.[15,37] Therefore, a change in the effective positive charge at the BChl center is expected to modify the orbital energies, via electrostatic interactions with the π electrons, by $\Delta E_{a_{2u}} \gg \Delta E_{e_{gy}} \sim \Delta E_{e_{gy}} > \Delta E_{a_{1u}}$, and the energy of the Q_x and B_y transitions will be modified to a much larger extent that of Q_y and B_x. Still, following this simple picture, Q_y and B_x are also expected to be somewhat modified, but in the opposite direction. This will be treated more elaborately considering configuration interaction among the individual single-electron promotions in the accompanying paper.

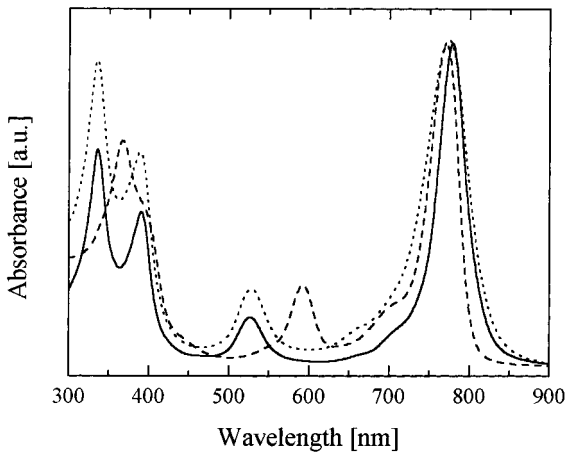

Figure 2. Absorption spectra of [Ni]-BChl in DE (—), acetonitrile (•••) and pyridine (– –).

Solvent Dependence of Optical Spectra. Any effect of the central metal on the energy of the four orbitals is expected to be additionally modulated by axial ligation of the central metal in [M]-BChl, because ligation probably reduces the effective charge of the central metal and hence its electrostatic interaction with the π electrons. In agreement with this, the spectra of BPhe, which cannot bind additional ligands because of the lack of a central metal, are nearly solvent-independent. Pronounced solvent shifts (1110 cm^{-1}) have, however, been reported for the Q_x band of BChl and have been related to a change from 5- to 6-fold coordination, i.e., to the presence of one or two axial ligands.[38,39] Changes in the transition energy of the Q_y band were much smaller. The B bands have not been investigated in previous studies, but here we observed a shift of 1270 cm^{-1} for the B_y band upon changing the solvent from DE to pyridine.[40] The large shifts of the BChl's Q_x and B_y transition energies and the absence of significant shifts in BPhe indicate that the spectral modifications reflect neither a change in the solvent refractive index nor differences in the polarity of the [M]-BChl excited states but rather changes in the metal coordination number (n_c).

The observations found for BChl are also relevant to the other [M]-BChls reported here, as long as the metal can aquire an n_c larger than four. For example, the Q_x and B_y bands of [Cu]-BChl and [Co]-BChl are red-shifted by (1090 ± 50) cm^{-1} and by (1450 ± 150) cm^{-1}, respectively, similar to the shifts observed for BChl itself. Although [Zn]-BChl, [Cd]-BChl, and [Mn]-BChl are less affected, the solvent-induced shifts of their electronic transition energies are significant (ΔE_{Q_x} = (525 ± 125) cm^{-1}; ΔE_{B_y} = (790 ± 100) cm^{-1}). Exceptionally large shifts were observed for [Ni]-BChl (ΔE_{Q_x} = 2100 cm^{-1}; ΔE_{B_y} = 2500 cm^{-1}, Figure 2) which probably reflects a change from n_c = 4 in DE to n_c = 6 in pyridine. This change is supported by its analogy to Ni-porphyrins[13,31,41] and ^{1}H NMR combined

(32) Rodgers, A.; Hartwich, G.; Scheer, H. Unpublished results, 1996.
(33) Takiff, L.; Boxer, S. G. *Biochim. Biophys. Acta* **1988**, *932*, 325−334.
(34) Warshel, A.; Parson, W. W. *J. Am. Chem. Soc.* **1987**, *109*, 6143−6152.
(35) Thompson, M. A.; Zerner, M. C.; Fajer, J. *J. Phys. Chem.* **1991**, *95*, 5693−5700.
(36) This labeling was derived for the D_{4h}-symmetric metal-substituted porphyrins but is applicable to chlorins and bacteriochlorins despite reduced symmetry.
(37) Scherz, A.; Fisher, J. R.; Braun, P. In *Reaction Centers of Photosynthetic Bacteria*; Michel-Beyerle, M. E., Ed.; Springer-Verlag: Berlin, 1990; pp 377−388.
(38) Evans, T. A.; Katz, J. J. *Biochim. Biophys. Acta* **1975**, *396*, 414−426.
(39) Callahan, P. M.; Cotton, T. M. *J. Am. Chem. Soc.* **1987**, *109*, 7001−7007.
(40) The B_x band, which normally shows as a shoulder at the low-energy side of the B_y band, in pyridine is too close to the B_y band to be resolved.

with CD spectra (vide infra). The only metal complex with little solvent effect on the Q_x and B_y transitions (<300 cm^{-1}) is [Pd]-BChl, due to the preferential 4-fold coordination of Pd[42] in all solvents.

As for [Ni]- and [Pd]-BChl, EXAFS measurements indicated a 4-fold coordination for [Zn]-BChl in DE.[23] It seems reasonable to assign a 4-fold coordination also to Cd-BChl in DE because of the chemical similarity of Cd and Zn. Tetracoordination for these complexes as well as for [Cu]- and [Co]-BChl in DE is also indicated by analogy to the [M]-porphyrins and -chlorins.[13,26,41]

The only M-BChl with established 5-fold coordination is for BChl (M = Mg) in DE. However, since pentacoordination of [Zn], [Cu], and [Co] in strong nucleophiles such as pyridine has been thoroughly documented[43] and is exhibited in [Zn]-, [Cu]-, and [Co]-porphyrins dissolved in pyridine,[41] we might expect that $n_c = 5$ for the respective [M]-BChls. The assignment of 5-fold coordination for [Zn]-BChl in pyridine is strengthened by the finding that it is also 5-fold coordinated in the bacterial reaction center.[23] There, the Q_x absorption band for this molecule is located at ~595 nm (16 800 cm^{-1}), which is red-shifted by 500 cm^{-1} with respect to the same transition in pyridine (17 300 cm^{-1}). This is similar to the environmentally induced red shift of (700 ± 200) cm^{-1} observed for BChl when its Q_x transition energy for pentacoordination in the reaction center is compared with the Q_x transition energy for pentacoordination in DE.[21,44] Thus [Zn]-BChl should be pentacoordinated in pyridine. Sixfold coordination is indicated only for [Mg]- and [Ni]-BChl in pyridine (vide supra).

Linear Correlation of Transition Energies with Scaled Metal Electronegativity χ^P_M/r^i_M. In the porphyrin and chlorin series, the influence of the central metals on the redox properties of the [M]-porphyrins and [M]-chlorins have been linearly correlated to the central metals' electronegativities (χ^P_M). It has been suggested that an increase in χ^P_M should cause a shift of the N-σ electrons toward the metal which would substantially lower the potential of the N-π and C-π electrons (inductive effect[45]). However, this approach failed to account for the experimental results in a rigorous manner.[46]

For [M]-BChls, a similar dependence of the redox properties[22] and especially of the optical transition energies presented here failed to provide good linear relationships unless the complexes were classified into three groups according to their coordination number. Attempts to relate changes in the Q_x and B_y transition energies of the complexes studied in each group with χ^P_M resulted in a moderate linear correlation (Table 3). The linearity within each group was improved, however, when χ^P_M was scaled by $1/r^i_M$ (where r^i_M is the ionic radius of the metal). This χ^P_M/r^i_M ratio had already been used by Buchler[13] as a criterion for the binding strengths of a variety of metals to porphyrins ("stability factor").

Intuitively, the normalization of χ^P_M to the ionic radius r^i_M serves as a scaling factor. This could relate to the special situation in BChl: Since the macrocycle and hence its central hole are of nearly fixed sizes, it cannot, like acyclic ligands, readily adapt to different sizes of the central metals, which vary both with the type of the metal and with its coordination (see below).

Table 3. Parameters for Linear Regression of the [M]-BChls' B_y and Q_x Transition Energy $E_{M,T}$ (Figure 2) at Central Metal Coordination Number n_c According to eq 1 ($E_{M,T}$ in cm^{-1}, r^i_M in 10^{-14} m, and χ^P_M Given in charge/m). Correlation Coefficient X_{corr}^2 Given for the Fits of the Respective Absorption Maxima vs the Expression underneath in Parentheses. Indices of *a* and *b* Given in eq 1 Are Left Out Here for Clarity

B_y Transition

n_c	$a \pm \Delta a$	$b \pm \Delta b$ [cm^{-1}]	X_{corr}^2 (χ^P_M/r^i_M)	X_{corr}^2 (χ^P_M)	X_{corr}^2 ($\chi^P_M/r^{i\,2}_M$)
4	1648 ± 157	24447 ± 461	0.982	0.875	0.972
5	816 ± 80	25612 ± 206	0.991	0.880	0.985
6[a]	531 ± 29	25788 ± 66	0.999	0.963	0.976

Q_x Transition

n_c	$a \pm \Delta a$	$b \pm \Delta b$ [cm^{-1}]	X_{corr}^2 (χ^P_M/r^i_M)	X_{corr}^2 (χ^P_M)	χ_r^2 ($\chi^P_M/r^{i\,2}_M$)
4	1156 ± 36	15095 ± 100	0.998	0.837	0.992
5	657 ± 106	15683 ± 265	0.963	0.863	0.972
6[a]	357	15690			

[a] Too few data points to justify linear regression; parameters are just shown for the sake of completeness.

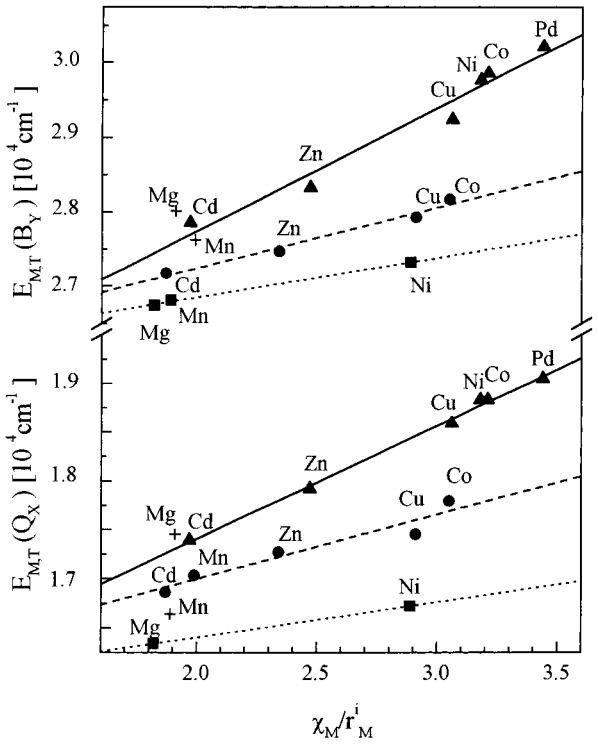

Figure 3. Correlation of the B_y (top) and Q_x transition energies (bottom) with χ^P_M/r^i_M of the BChl's central metal (indicated in the figure). Coordination numbers n_c: (△) $n_c = 4$, (—) linear fit; (●) $n_c = 5$, (– –) linear fit; (■) $n_c = 6$, (···) linear fit (see text for details).

The empirical correlation found for [M]-BChls (Figure 3 and Table 3) reads as

$$E^{n_c}_{M,T} = a^{n_c}_T \frac{\chi_M}{r^i_M} + b^{n_c}_T \qquad (1)$$

where the parameters $a^{n_c}_T$ and $b^{n_c}_T$ are characteristic of a

(41) Scheidt, W. R. In *The Porphyrins*; Dolphin, D., Ed.; Academic: New York, 1979; Vol. III, pp 463–512.

(42) The d^8-metal Pd^{2+} is known to exhibit only quadratic planar coordination in porphyrins (ref 13).

(43) Cotton, F. A.; Wilkinson, R. *Advanced Inorganic Chemistry*; Wiley: New York, 1988; 5th ed.

(44) Scheer, H.; Struck, A. In *The Photosynthetic Reaction Center*; Norris, J. R., Deisenhofer, J., Eds.; Academic Press: New York, 1993; pp 157–192.

(45) Gouterman, M. *J. Chem. Phys.* **1959**, *30*, 1139–1160.

(46) Fuhrhop, J. H.; Kadish, K. M.; Davis, D. G. *J. Am. Chem. Soc.* **1973**, *95*, 5140–5152.

particular coordination number n_c and transition "T" but are independent of the incorporated metal.

In the accompanying manuscript[28] this relationship will be explored following Mulliken and others[43,47,48] who claimed that electronegativity (i) depends on the metal's particular environment and valence state and (ii) represents an electrostatic potential induced by an effective positive charge Q_M at the metal atom center. We propose that by changing the metal coordination number (n_c) we modify the metal electronegativity. This effect is moderated by the particular π orbital because each orbital contains nitrogen centers that are coordinated with the metal. Further, a decrease in the metal ionic radius (r^i_M) decreases the orbital overlap of the metal with the nitrogens, and thereby the screening of the effective positive charge. In light of these considerations, the first term $a^{n_c}_T$ in eq 1 represents the change in a particular transition energy due to a change in metal electronegativity within the BChl frame, while the second term $b^{n_c}_T$ represents a reference transition energy. The physical meaning of $a^{n_c}_T$ will be clarified in the subsequent paper[28] where we shall also derive the effective positive charge for each of the substituting metals. The empirically derived variable χ^P_M/r^i_M is linearly related to the actual effective charge Q_M of the central metal.

This treatment also provides a rationale for scaling χ^P_M in the frame of the "rigid inner hole" discussed above: As the metal's ionic radius decreases, the overlap between the metal orbitals and those of the nitrogens decreases, and this is expected to decrease the screening of the metal's effective charge (and to increase the ionic character of the bond). To roughly compensate for this effect with varying sizes of the central metal, it seems sufficient to scale χ^P_M by $1/r^i_M$. Qualitatively, this scaling can also correct for metals being too large to fit into the inner hole of the porphyrin by decreasing the effective charge as compared to coplanar complexes. Here, only Cd^{2+} qualifies for such a sitting-atop complex, which does not allow for a quantitative evaluation.

A similar rationale may account for the need to group the [M]-BChls studied according to n_c before establishing the relationships with χ^P_M/r^i_M. Each additional ligand increases the shielding of the metal's nucleus (note that r^i_M increases with n_c and that this increase is accounted for in the empirical correlation). In these groups, the spectra of [Pd]-, [Ni]-, [Co]-, [Cu]-, and [Zn]-BChl in DE can be used to define the correlation between these transitions and χ^P_M/r^i_M for tetracoordinated [M]-BChls. Note that the B_y and Q_x transition energies of [Cd]-BChl fit into this correlation very well (Figure 3). This observation supports the assignment of a 4-fold coordination to [Cd]-BChl in DE.[50]

The Q_x and B_y transition energies of [Cu]-, [Co]-, [Zn]-, and [Cd]-BChl in pyridine show a different but linear correlation with χ^P_M/r^i_M (Figure 3). As discussed previously, these complexes are probably 5-fold coordinated in pyridine. Since the slopes of the linear correlations for 4- and 5-fold coordination are different, the comparatively small solvent shifts of the B_y and Q_x transitions for [Zn]- and [Cu]-BChl (vide supra) are due to their low χ^P_M/r^i_M values. Finally, the Q_x transition energy of [Mg]-BChl in pyridine has been shown to relate to its 6-fold coordination.[38] [Ni]-BChl in pyridine should also exhibit 6-fold coordination, so that these and the corresponding B_y transitions can serve to define a third line that correlates 6-fold coordinated [M]-BChls with their χ^P_M/r^i_M values (Figure 3).

The linear correlations between the Q_x or B_y transition of [M]-BChls and χ^P_M/r^i_M (grouped by coordination numbers) are consistently better than those with χ^P_M and, although to a lesser extent, with $\chi^P_M/r^i_M{}^2$ (Table 3). The largest deviations from linear correlation with χ^P_M/r^i_M are given for [Mn]-BChl in DE or pyridine and [Mg]-BChl in DE. The Mn "anomaly" may reflect the presence of oxygen-bridged [Mn]-BChl dimers in equilibrium with monomers,[17] which may influence the two transitions differently. There is no evidence that [Mg]-BChl in DE forms such dimers. However, since it is known to exhibit 5-fold coordination (while lying on the line of 4-fold coordination), its χ^P_M/r^i_M value in the 5-fold coordination may be underestimated by approximately one-third. A very similar deviation is obtained for [M]-BChls in the $B_{A,B}$ (= "monomeric") binding sites of purple bacterial reaction centers, where a 5-fold coordination has been proven.[23,51,52] The protein supposedly imposes a fixed geometry on the complex, although the 3-acetyl group of the nearby BPhes could be regarded as a potential additional candidate for ligation, or at least for influencing the central metal of the monomeric [M]-BChls. In this environment, [Mg]-BChl, [Zn]-BChl, and [Ni]-BChl show Q_x transitions at 600, 595, and 585 nm, respectively.[17,18,24] The correlation of this transition with χ^P_M/r^i_M for [Zn]- and [Ni]-BChl shows a a^{nc}_{Qy} value identical to the one obtained for the 5-fold coordinated [M]-BChls in solution (vide infra), but again the χ^P_M/r^i_M value for [Mg]-BChl is underestimated by approximately one-third. The obvious deviation of Mg, which is of central biological importance, needs to be further explored. Note that Mg is the only metal studied that lacks d orbitals, and therefore $p\pi-d\pi$ electron donation from and $d\pi-p\pi$ backbonding to the axial ligands might be different.

The influence of electron donation from an additional axial ligand on χ^P_M is illustrated by the decreasing slope with increasing coordination number (Table 3). Since the influence on r^i_M is accounted for, adding the first axial ligand reduces χ^P_M/r^i_M (and thus Q_M) by approximately 40% (Q_x) to 50% (B_y), whereas the second axial ligand induces only a reduction of 25% (Q_x) to 20% (B_y) relative to $n_c = 4$.[53]

As shown in Figure 3 and Table 3, a^{nc}_{By} is larger than a^{nc}_{Qx}. In a zero-order approximation neglecting configuration interaction, this indicates either a larger admixture of e_{gx} to the Q_x transition than of e_{gy} to the B_y transition, or a stronger effect of the central metal on e_{gx} than on e_{gy}. A semiquantitative estimate of the central metals' influence on the individual orbital energies is provided by electrochemical data of the [M]-BChls in THF,[22]

(47) Mullay, J. In *Structure and Bonding*; Sen, K. D., Jorgensen, C. K., Eds.; Springer-Verlag: Berlin, 1987; Vol. 26, pp 1−26.

(48) Alonso, J. A.; Balbas, L. C. In *Structure and Bonding*; Sen, K. D., Jorgensen, C. K., Eds.; Springer-Verlag: Berlin, 1987; Vol. 26, pp 41−78.

(49) Harrison, R. D. *Datenbuch Chemie Physik*; Vieweg & Sohn: Braunschweig, 1982.

(50) The attribution of n_c to [Cd]-BChl may be disturbed because Cd^{2+} may not fit into the inner hole of the macrocycle and thus, deviate from the other [M]-BChls.

(51) Deisenhofer, J.; Epp, O.; Miki, K.; Huber, R.; Michel, H. *Nature* **1985**, *318*, 618−624.

(52) Ermler, U.; Fritzsch, G.; Buchanan, S. K.; Michel, H. *Structure* **1994**, *2*, 925−936.

(53) A coordination number n_c of four is likely for most of the [M]-BChls examined electrochemically in tetrahydrofurane according to their Q_x absorption (ref 22).

(54) There is, within the error of the correlation, no change in the constant, if n_c changes from five to six. The solvent for both coordination situations is pyridine. When n_c changes from four to five the constant experiences a weak relative increase (<5% for B_y or Q_x). The change from 4- to 5-fold coordination is accomplished by a solvent change from DE to pyridine for almost all [M]-BChls. However, such an increase is very sensitive to minor changes in the slope of the respective correlations. Thus it is better to judge the pure solvent effect on the constant from BPhe and [Pd]-BChl, which have no axial ligands in every solvent, but their Q_x and B_y transition energies are lowered by approximately 300 cm^{-1}.

where according to the Q_x transitions, most of the complexes are tetracoordinated.[54] There, the redox potentials are also linearly correlated with χ^P_M/r^i_M. The potentials $E_{1/2}$ vs Ag/AgCl for the oxidation and reduction exhibit a slope of −1300 (HOMO, a_{1u}) and −1360 (LUMO, e_{gx}), respectively, in agreement with the minor variability of the Q_y transition in the series of examined [M]-BChls. Comparison with a^{nc}_T for the B_y ($a_{2u} \rightarrow e_{gy}$) and Q_x ($a_{2u} \rightarrow e_{gx}$) transitions of ∼1650 and ∼1150, respectively, for $n_c = 4$ enables estimating the orbital shift per unity of χ^P_M/r^i_M and yields $\Delta E_{a_{2u}} \approx -2500$ cm^{-1}, $\Delta E_{e_{gx}} \approx -1360$ cm^{-1}, $\Delta E(a_{1u}) \approx -1300$ cm^{-1} and $\Delta E_{e_{gy}} \approx -850$ cm^{-1}. On the basis of this estimate, the difference between a^{nc}_{By} and a^{nc}_{Qx} can be attributed to a stronger effect of the central metal on e_{gx} than on e_{gy}.

^{1}H NMR Measurements. No ^{1}H NMR signals were obtained for the paramagnetic complexes [Co]-, [Cu]-, and [Mn]-BChl because of extensive line broadening. [Ni]-BChl showed broad lines in pyridine, indicating a paramagnetic, octahedral complex; however, it is diamagnetic in CH_3CN (sharp lines) and probably square-planar-coordinated. Although quadratic pyramidal [Ni]-complexes ($n_c = 5$) can exhibit paramagnetic high-spin as well as low-spin configurations, we disfavor 5-fold coordination in any of the solvents because of the shift in the Q_x transition (531 nm in CH_3CN and 598 nm in pyridine, Figure 2) and the dependence on n_c derived above. The assignment of $n_c = 4$ in CH_3CN and $n_c = 6$ in pyridine is supported by EXAFS measurements.[23] The central metal of [Ni]-BChl in reaction centers is 5-fold-coordinated, showing a Q_x absorption at ∼585 nm. [Ni]-BChl with $n_c = 5$ in solution should then absorb around 560 nm, if the environmentally induced red shift is taken into account.

The ^{1}H NMR signals of selected protons of the diamagnetic complexes in the [M]-BChl series are listed in Table 2. In general, the chemical shift decreases for a given proton of the pyridine-solvated [M]-BChls (M = Pd, Zn-, Mg-, and Cd) with decreasing χ^P_M/r^i_M values.[55] This agrees with the electron-withdrawing effect (−I effect) of the central metal that leads to deshielding of the protons and thus to a low-field shift. Of particular interest are the meso protons (5-, 10-, and 20-H), which are closest to the π system and show the largest ring-current shifts. The more distant protons such as 17-H, 18-H, 2-CH_3, and 13^2-CO_2CH_3 are influenced less, but the general direction is the same. This is qualitatively consistent with the electrostatic effect of the central metal on the ring current of the π system.

On the basis of this assignment, the increasing chemical shifts with a decreasing −I effect (χ^P_M/r^i_M value) for the 13^2-proton and the 12-CH_3-protons are unexpected. They may be rationalized as a result of the involvement of (partial) enolization for the [M]-BChls. Although significant populations of the enol form of the β-ketoester system of the isocyclic ring V (probably a 13^1-en-13^1-ol form) have never been detected by ^{1}H NMR measurements of [Mg]-BChl,[56,57] the H exchange at 13^2-H as well as epimerization at this chiral position have been explained by keto−enol tautomerism.[57,58] A reduced π-electron density could stabilize the transition state to the enol form by a reduced overlap of the developing (negatively charged) π orbital at position C-13^2 with the neighboring π orbitals. The relative contribution of the enol form and therefore the mean electron density at position 13^2 is increased. This would result in an increased screening (decreased chemical shift) for the proton at position C-13^2 with increasing χ^P_M/r^i_M values. Vinylogous enolization, used for explaning the H^1/H^2 exchange at 12-CH_3 in BChl,[59] would copy the behavior of the proton at C-13^2 to the protons 12-CH_3 (and potentially even to 3-$COCH_3$).

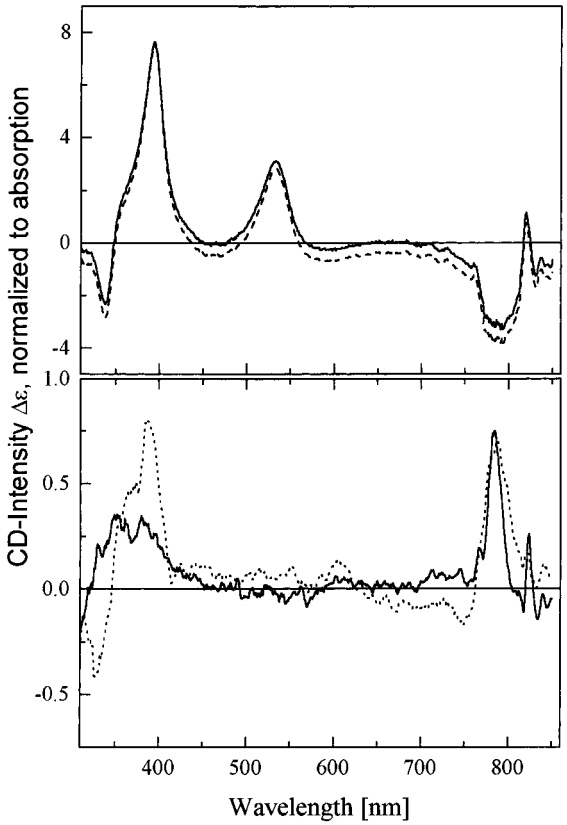

Figure 4. Circular dichroism spectra, normalized to identical optical density at the Q_y transition. Upper trace: [Ni]-BChl in DE (—) and acetonitrile (− − −). Lower traces: [Ni]-BChl in pyridine (—); [Mg]-BChl in DE (···). Note that *Y* scales differ by a factor of 8. The spike at ∼823 nm is an artifact from the Xe lamp.

Circular Dichroism. The CD spectrum of [Ni]-BChl in pyridine has signs and intensities similar to those of BChl (Figure 4, bottom) and all the other [M]-BChls including the square-planar [Pd]-BChl (not shown). Such a CD signal is expected for a roughly planar macrocycle with octahedral Ni. In contrast, the CD signals for [Ni]-BChl in CH_3CN or DE are ∼10-fold stronger (Figure 4, upper trace) than those of all the other complexes in the series. This strong increase in CD intensity probably reflects S_4 ruffling of the macrocycle typical for square-planar, low-spin [Ni]-iso-bacteriochlorins,[60] which renders the macrocycle inherently dissymmetric.

The change from planar to S_4 ruffling is probably related to the small ionic radius of low-spin Ni^{2+} (∼60 pm, compared to ∼70 pm with high-spin) that shortens the [Ni]−N bond length. However, there is no concomitant change in the Q_y transition energy. Connick et al.[61] observed a 525 cm^{-1} red shift in Q_y for a similar high-spin/low-spin transformation in a [Ni]-tris-

(55) ^{1}H NMR of [Ni]-BChl in C^2H_3CN is not included into this comparison, since the chemical shifts of [M]-BChls are strongly dependent on the solvent.

(56) Scheer, H.; Katz, J. J. *J. Am. Chem. Soc.* **1978**, *100*, 561−571.
(57) Watanabe, T.; Machida, K.; Suzuki, H.; Kobayashi, M.; Honda, K. *Coord. Chem. Rev.* **1985**, *64*, 207−224.
(58) Dougherty, R. C.; Strain, H. H.; Katz, J. J. *J. Am. Chem. Soc.* **1965**, *87*, 104−115.
(59) Scheer, H.; Norris, J. R.; Katz, J. J. *J. Am. Chem. Soc.* **1977**, *99*, 1372−1381.
(60) Senge, M. O.; Smith, K. M. *Photochem. Photobiol.* **1991**, *54*, 841−846.
(61) Connick, P. A.; Haller, K. J.; Macor, K. A. *Inorg. Chem.* **1993**, *32*, 3256−3264.

β-oxoporphyrin (formally a dihydro-bacteriochlorin) and a 306 cm^{-1} blue shift in a [Ni]-bis-β-oxoporphyrin (formally an isobacteriochlorin), whereas Fajer et al.[10] reported a much larger red shift of ~1350 cm^{-1} for the Q_y transition upon distortion of a Zn-porphyrin (with unchanged spin state). This may indicate that the high-spin to low-spin change alone causes a blue shift which is (almost) canceled in [Ni]-BChl by the concomitant distortion.

Conclusions

Metal-substituted bacteriochlorophylls provide a wealth of spectroscopic data, which, because of the band's overlap, is not readily available from porphyrins or chlorins. The series of [M]-BChls was used to test the influence of the central metal as well as the presence of additional axial ligands on the energies of the four lowest electronic transitions, B_y, B_x, Q_x, Q_y, in the framework of the four-orbital model. Because of the fixed geometry of the macrocycle, much of the data gave satisfactory linear correlations with χ_M^P/r_M^i rather than with χ_M^P alone. There, r_M^i serves as a scaling parameter and χ_M^P/r_M^i accounts for the effective charge of the central metal in the fixed frame of the macrocycle. Yet, further scaling is needed to account for the effect of the metal valence state and axial ligation. This is achieved by grouping [M]-BChls according to their (putative or experimental, when available) coordination number. For those χ_M^P/r_M^i correlations using χ_M^P values that do not account for different coordinations per se, axial ligands can be regarded as a factor that mainly reduces the effective charge and thus the electronegativity of the central metal. The ratio χ_M^P/r_M^i is therefore a useful heuristic parameter in relating spectral and redox properties in the conformationally restricted macrocyclic complexes. Alternatively, the ligand effect may be accounted for by using the concept of equalization of electronegativities.[62] If successful, this approach may enable considering linear relationships as mentioned above without preclassification of the coordination or metal valence state. Thus, in view of the changing concepts of electronegativity, a more rigorous approach is desirable. Such a concept is outlined in the subsequent manuscript,[28] which is based solely on electrostatic interactions of the central metal with the frontier orbitals of the macrocycle.

Experimental Section

7a was isolated from *Rhodobacter sphaeroides* using standard methods.[44,63,64] Hydroxylation at position C-13^2 to yield **7b** was done by storage of **7a** in methanol for 5 days in the dark and subsequent silica gel chromatography;[63,65] C-13^2-decarbomethoxylation was achieved by 12 h of reflux in pyridine.[63,66] Demetalation of **7a** (**7b**) was achieved by treatment with small amounts of glacial acetic acid to yield **1a** (**1b**).[67]

Direct Metalations by Acetate/DMF. 8a (**8b**) was prepared by refluxing **1a** (**1b**), (~70 μM) in dimethylformamide, with a 300-fold excess of anhydrous $Cd(OAc)_2$ for 40 (60) min at 130 °C. The reaction was followed spectroscopically and run to completion. The crude products were isolated by partition between DE and $NaHCO_3$-saturated water and purified on silica gel (1.5% Na-ascorbate admixed) with toluene/acetone/triethylamine (88/10/2; v/v/v); yield ~85%.

6a (**6b**) was prepared by refluxing **1a** (**1b**), (~70 μM) in dimethylformamide, with a 1000-fold excess of anhydrous $Zn(OAc)_2$ for 60 (75) min at 110 °C (reflux at 163 °C decreases the reaction time to 5 min). The reaction was followed spectroscopically and run to completion. Isolation and purification of products was done as for **8a**,**b** (yield ~80%). Metalation by the acetate/DMF method can be extended to other derivatives of BPhe, when reaction conditions are slightly varied. For instance, metalation of 3-vinyl-BPhe or 3-vinyl-13^2-hydroxy-BPhe with $Zn(OAc)_2$ proceeds under identical conditions within ~40 min at 120 °C.

Direct Metalations by Acetate/Acetic Acid. 6a (**6b**) was prepared by refluxing **1a** (**1b**) or **7a** (**7b**), (~70 μM) in glacial acetic acid, with a 250-fold excess of anhydrous $Zn(OAc)_2$ and 50 mM sodium ascorbate for 120 (30) min at 100 °C. The acetic acid was then evaporated in a stream of N_2, and the Zn complex was extracted with diethyl ether and purified on a preparative ModCol HPLC column (250 × 25.4 mm) packed with Bakerbond Silica NP (particle size 10 μm; pore diameter 150 Å). **6a** was eluted isocratically (10 mL/min) with a mixture of 2-propanol (5%), methanol (5%), and *n*-hexane (90%, v/v) with a retention time of about 17 min, with ~75% yield of the purified compound. **6b** was purified by column chromatography on silica gel, using the same solvent mixture as for HPLC, giving a yield of 90−95%. The Zn-derivative of 13^2-decarbomethoxy-BPhe (or 13^2-decarbomethoxy-BChl) can be obtained under the same conditions; reaction time is 30 min at 100 °C; isolation and purification is identical to that of **6b**.

5a was prepared by refluxing **1a** or **7a**, (~70 μM) in glacial acetic acid, with a 250-fold excess of anhydrous Cu_2O and sodium ascorbate (50 mM) for 15 min at 100 °C. **5b** is formed at ambient temperature by mixing **1b** or **7b**, (~70 μM) in glacial acetic acid, with a 250-fold excess of anhydrous Cu_2O and 50 mM sodium ascorbate. The Cu derivative of 13^2-decarbomethoxy-BPhe (or 13^2-decarbomethoxy-BChl) was obtained at conditions identical to those described for **5b**. Despite using Cu_2O, the Cu^{2+} complexes were always formed due to the presence of residual oxygen or disproportionation. Isolation and purification was done as described for the Zn^{2+} complexes prepared by the glacial acetic acid method, yielding ~75% (**5a**), ~90% (**5b**), and ~90% (Cu derivative of 13^2-decarbomethoxy-BChl).

Transmetalation. Addition of metal chlorides to a solution of the Cd complexes **8a** or **8b** (~60 μM) in acetone resulted in transmetalation to **2a**,**b**−**6a**,**b** and **9a**,**b**. The reactions were carried out under strict Ar protection and ran to completion. The metal chlorides were added at a 10-fold molar excess (**5a**,**b** and **6a**,**b**), 100-fold molar excess (**3a**,**b**), or to saturation (**2a**,**b**, **3a**,**b**, and **9a**,**b**). The reactions occurred practically instantaneously at 298 K, except for **2a**,**b** and **4a**,**b** (~30−40 min reflux) and were followed spectroscopically. Small amounts of C7−C8-oxidized products (λ_{max} ~ 680 nm) were formed due to the presence of residual oxygen which can be suppressed by adding Na-ascorbate (saturated). Isolation and purification of the products was done as for **8a**,**b**, yielding 90−95% of pure product. Absorption, emission, the molecular ion of the mass spectra, and the main signals of the ^{1}H NMR spectra are listed in Tables 1 and 2. Full spectra are available as Supporting Information.

Instrumentation. UV/vis absorption spectra were recorded on a Perkin-Elmer Lamda 2 spetrophotometer. Fluorescence emission spectra were determined with a Spex Fluorolog 221 equipped with a 450-W xenon lamp and were normalized to the sensitivity of the photomultiplier tube and excitation energy. Maximum optical densities for fluorescence measurements were <0.1 cm^{-1} and excitation was into the Q_x absorption band of **1a**,**b** to **9a**,**b**. Circular dichroism spectra (CD) were recorded on a Dichrograph CD6 (Jobin Yvon). Fast atom bombardment mass spectra (FAB-MS) were recorded on a CH7a/SS 100 mass spectrometer (Varian MAT) or a Finigan MAT 9000 with a Cs gun. Liquid-surface ionization was done in a matrix of *m*-hydroxybenzyl alcohol. ^{1}H NMR spectra were recorded on a 360-MHz Bruker, model AM360. Standard solvent was pyridine-d_5, and chemical shifts are in ppm against tetramethylsilane as internal standard. Extinction coefficients were determined by ICP/ICPMS atom absorption spectra (AAS) of the central metals; before combustion, the solvent in samples of **1a**,**b** to **9a**,**b** with quantified optical densities was first

(62) York, D. M. *Int. J. Quantum Chem.* **1995**, Suppl. 29.
(63) Struck, A.; Cmiel, E.; Katheder, I.; Schäfer, W.; Scheer, H. *Biochim. Biophys. Acta* **1992**, *1101*, 321−328.
(64) Omata, T.; Murata, N. *Plant Cell Physiol.* **1983**, *24*, 1093−1100.
(65) Schaber, P. M.; Hunt, J. E.; Fries, R.; Katz, J. J. *J. Chromatogr.* **1984**, *316*, 25−41.
(66) Pennington, F. C.; Strain, H. H.; Svec, W. A.; Katz, J. J. *J. Am. Chem. Soc.* **1964**, *86*, 1418−1426.
(67) Rosenbach-Belkin, V. Ph.D. Thesis, The Weizmann Institut of Science, Rehovot, Israel, 1988.

evaporated in quartz glass tubes and the samples then treated with concentrated nitric acid to allow complete release of the metal.

Acknowledgment. Work was supported by the Deutsche Forschungsgemeinschaft (AZ Sche 140/9-2,3 and SFB 143, TP A9) and the Willstätter-Avron-Minerva foundation for photosynthesis. We thank Dr. P. Schraml (GSF, München-Neuherberg) for atomic absorption measurements.

Supporting Information Available: Listings of experimental procedures and spectra of Table 2 (absorption, fluorescence, ^{1}H NMR, FAB-MS), additional absorption spectra in pyridine, [CD] spectra, and electron density distribution for BChl (adapted from ref 37) (65 pages). See any current masthead page for ordering information and Web access instructions.

JA970874U